

# Coupling in Fe(2 ML)/V( $y$ ML) and Fe(2 ML)/V( $y$ ML)/Fe(3 ML)/V( $y$ ML) ( $y \geq 4$ ) superlattices

Karen B. Paul\*

*Institut für Physik, Bereich für Experimentalphysik,  
Karl-Franzens-Universität,  
8010 Graz, Austria*

Received 9 August 2006; accepted 7 November 2006

---

**Abstract:** Fe(2 ML)/V( $y$  ML) and interleaved Fe(2 ML)/V( $y$  ML)/Fe(3 ML)/V( $y$  ML) superlattice systems with spacer thicknesses,  $y$ , ( $4 \leq y \leq 17$ ) were investigated macro-magnetically to estimate the coupling strength and the magnetoresistance in these materials, and particularly in the antiferromagnetically coupled monolayers. The results from the magnetic and magnetoresistive measurements indicate that adding one monolayer of Fe increases the antiferromagnetic coupling and the magnetoresistivity ratio from 0.0075 mJ/m<sup>2</sup> at 20 K and 2 % at 10 K for Fe(2 ML)/V( $y$  ML), to 0.05 mJ/m<sup>2</sup> and 2.5 % for Fe(2 ML)/V( $y$  ML)/Fe(3 ML)/V( $y$  ML) at the same temperatures. Both systems exhibit in-plane magnetic and magnetoresistive isotropy, therefore the increase of the conferred physical parameters is attributed mainly to the stresses at the interface as governing mechanisms over the magnetoelastic forces.

© Versita Warsaw and Springer-Verlag Berlin Heidelberg. All rights reserved.

*Keywords:* Supperlattice, interlayer exchange coupling, magnetic anisotropy energy, heterostructure, ferrimagnetism

*PACS (2006):* 75.70.Ak; 75.30.-m, 75.30.Fv

---

## 1 Introduction

Research on two ferromagnetic (FM) metals with thicknesses in the monolayer (ML) range, separated by a nonmagnetic (NM) spacer has been a topic of extensive theoretical [1] and experimental [2] work for these structures' potential in giant magnetoresistive (GMR) devices [3], hydrogen storage [4] and recording media [5]. Theoretical studies

---

\* E-mail: dr.\_kpaul@hotmail.com

and experimental data deal with FM/noble metal/FM [1, 2], FM/rare earth/FM [6] and FM/AF/FM [7, 8] architectures. (AF  $\equiv$  antiferromagnetic.) The Ruderman - Kittel - Kasuya - Yosida (RKKY)-like interlayer exchange coupling (IEC) in FM/NM/FM multilayers is periodic with diminishing amplitude at each consecutive period [1, 9]. The IEC is temperature dependent and its highest values are at the lowest temperatures [1]. They depend on the Fermi surface of the spacer, and not on the FM materials [1]. The IEC may be modified by the capping layer of the structure [10].

A majority of works discuss the period of the oscillation in the IEC and its amplitude [1, 8]. First principles calculations on the exchange coupling in magnetic Fe/V and Fe/Cr multilayers predict short and long oscillation periods of 3 and 11 ML for (001)Fe/V, and  $\sim 2$  and 12 ML for [001]Fe/Cr [9]. These values are dependent on the parameters in the calculation - e.g. step potential in Ref. [9]. Broadly concluded, two ferromagnetic layers separated by a nonmagnetic spacer can be AF coupled at a specific narrow range of spacer thicknesses. The theoretically calculated coupling energy densities at 0 K are  $\approx 0.3 \text{ mJ/m}^2$  for Co/NM/Co and  $0.4 \text{ mJ/m}^2$  for Ni/Cu/Ni [1], therefore a considerable magnetoresistive effect is anticipated in these heterostructures. The experimentally observed values of the coupling energy densities and the magnetoresistance ratio (MR), however, are often very different from the calculated ones [2]. The divergences are usually attributed to specifics of the fabrication and imperfections at the interface, such as roughness [1], interdiffusion and islands [11], alloying [12]. There are not so many works, which consistently investigate the effect of the fabrication procedure on the performance of the device; the data on this problem strive for further understanding and optimization of the outcome. And there are only a few works on the effect of the magnetic anisotropy (MA) on the coupling strength in Fe/V systems [13–15]. (The MA in this work reflects jointly the magnetoelastic coupling of the FM layers, the shape anisotropy, and the strains and stresses at the interfaces.)

It is established, that the Fe(x)/V(y)/MgO(001) materials are magnetized in-plane and the magnetic anisotropy becomes relevant above 3 ML of Fe [13–15]. The corresponding samples may show spin reorientation of the Fe monolayers to the [110] direction [13, 14]. While for small Fe thicknesses the strains govern the growth [13], this is not so for  $\text{Fe} > 3$  ML. The thick Fe monolayers relax in the energetically more favorable [110] direction, thus causing a decrease of the IEC and the MR [14]. In a number of works [14, 15] it is verified that the coupling strength and the magnetoresistance have maximum values at  $\approx 5.5$  Fe monolayers and when antiferromagnetically coupled at 13 ML of V (see e.g. Fig. 2 in Ref. [15] b). However, the magnetic anisotropy deteriorates greatly the performance of the device - while for Fe(5 ML)/V(13 ML) at 10 K the MR is 5.2 % and the coupling strength  $\approx 0.09 \text{ mJ/m}^2$ , these parameters are practically the same in Fe(6 ML)/V(13 ML) and decrease dramatically upon further increase of the Fe coverage [15].

This work studies some isotropic materials within the Fe(x)/V(y)/MgO(001) system: Fe(2 ML)/V(y), 2 and 3 ML of Fe interleaved as Fe(2 ML)/V(y ML)/Fe(3 ML)/V(y ML), and Fe(3 ML)/V(y). (With x is denoted the Fe coverage and with y - the V spacer with thicknesses between 4 and 17 MLs.) Fe(3 ML)/V(y ML) is basically studied in Refs.

[15, 16], we will review some of the results as complementary to our conclusions. In a model isotropic system, the IEC and MR will increase in a specific way, and possibly linearly, with Fe thickness. In reality this will apply to a device when the Fe coverage is low and the surface/interface and shape anisotropies are approximately constants, which is the case. Thus the investigation leads to a quantitative estimate of the role of one Fe ML in an idealized Fe(x ML)/V(y ML)/MgO(001) device.

## 2 Experimental

The materials were prepared in a 3 source sputtering system, described in detail in Ref. [17]. To enhance the magnetic signal they were deposited as twenty five bilayer sequences of Fe(2 ML)/V(y ML) and ten repetitions of Fe(2 ML)/V(y ML)/Fe(3 ML)/V(y ML). The MgO(001) substrates, purchased from Sci Engineered Materials Inc., were pre-cleaned ex-situ and in-situ in the UHV system by Ar sputtering at 700° C and outgassing at this temperature for 15 min [16, 17]. The principal materials were deposited at 330° C - the optimal temperature for their epitaxial growth [16, 17]. The thicknesses of the layers were controlled during the deposition with a calibrated microbalance positioned close to the substrate. Additionally, they were verified by Rutherford Backscattering (RBS) measurements [18]. The samples were coated with a protective 30 Å Pd layer for measurements outside the vacuum chamber.

The structural quality of the samples was determined by  $\theta - 2\theta$  X-ray Diffraction (XRD) measurements made with a D5000 Siemens diffractometer using Cu  $K\alpha$  radiation. The experiments were carried out in a low-angle,  $2\theta = 1 - 14^\circ$ , and high-angle,  $2\theta = 50 - 85^\circ$ , ranges. The low-angle XRD data are used to calculate the repeat distances  $\Lambda$  and the average interface roughness; in the case, the average estimated roughness was  $\leq 1$  ( $\simeq 0.5$  ML). The high-angle XRD data are needed to determine the average out-of-plane lattice constants in the Fe and V layers. Software programmes were used to determine the discussed parameters: WinGixa [19] for the low-angle, and SUPREX [20] for the high-angle diffraction patterns.

The magnetic characterization of the materials was made with a Quantum Design Magnetic Property Measurement System (QD MPMS - 5). The magnetic performance of the two series of samples was monitored, and macroscopic parameters were determined to review their evolution with the thickness of the V spacer,  $N_V$ . The dc measurement-techniques are described in details in e.g. Ref. [21]: zero-field cooled and field-cooled magnetization  $M_{ZFC/FC}(T, H = const.)$  to estimate the temperature of the phase transition to the paramagnetic state,  $T_c(N_V)$ , hysteresis loops at fixed temperatures to determine the coercivity and its temperature dependence,  $H_c(T, N_V)$ , the saturation magnetization,  $M_s(T, N_V)$ , the saturation field,  $H_s(T, N_V)$ , the magnetic remanence,  $M_r(T, N_V)$ . (The temperature is denoted by T and the applied dc magnetic field by H in the discussion herein.) The AF samples in Fe(2 ML)/V(y ML) were studied by neutron reflectivity measurements made in Grenoble (France), because their MPMS-signals are very low as acceptable data. The transition temperature-points were calculated in two ways: as the

minimum of the derivative  $dM_{FC}(T)/dT$  and from the linear approximation after the inflection point of  $M^2(T) \rightarrow 0$  according to the mean field theory [2, 21].

The static dc magnetic measurements confirmed that these materials are magnetized in their planes only. Thus the samples in the magnetotransport measurements were aligned with their planes parallel to the magnetic field. The magnetoresistance was measured by the four-probe dc mode with in-plane electric current being parallel or perpendicular to the H, to observe a possible in-plane magnetoresistive anisotropy. The magnetic field was swept up and down to  $\pm 0.35$  T to ensure a complete magnetic saturation in the structures. (The dc magnetic measurements revealed saturation fields of approximately 0.3 T for the AF samples.)

### 3 Results and discussion

#### 3.1 Macroscopic magnetic characterization of Fe(2 ML)/V(y ML) and Fe(2 ML)/V(y ML)/Fe(3 ML)/V(y ML)

Both systems exhibited in-plane magnetizations and in-plane magnetic isotropy, i. e. the magnetic properties measured in 2 or more in-plane directions did not show observable differences within the experimental error; moreover, the magnetic signals measured out-of-plane were within the noise of the instrument. In Figs. 1 (a) and (b) are shown the transition temperatures of the materials as functions of the thicknesses of the V spacers.

Fig. 1 (a) depicts the variation of  $T_C(N_V)$  for Fe(2 ML)/V(y ML) and Fig. 1 (b) - for Fe(2 ML)/V(y ML)/Fe(3 ML)/V(y ML). The magnetization plots, either  $M_{ZFC}(T)$  or  $M_{FC}(T)$ , were measured in an applied field of 1200 A/m (15 Oe), linear for all temperatures accessible by the experiment, and the transition temperatures were estimated as described above. The  $T_C$ -values determined by the  $M^2 \rightarrow 0$  - plots released systematically higher values due to the method of calculation.<sup>†</sup> This, however, is irrelevant for the qualitative conclusions in regard to the coupling of the Fe monolayers. The measurements and the results for  $T_C$  revealed three types of coupling between the Fe layers: ferromagnetic, antiferromagnetic and uncoupled Fe layers. For the Fe(2 ML)/V(y ML)/Fe(3 ML)/V(y ML) system, the antiferromagnetic coupling generates ferrimagnetic behavior, as the magnetic moment of Fe(3 ML) is larger than that of Fe(2 ML), and there will be a resultant magnetic moment in the opposite alignment of the sublayers.

We invoke the mean field theory as a simplified theoretical background for interpreting the results in Fig. 1. According to it,  $T_C$  is proportional to the interlayer exchange energy per magnetic atom,  $\epsilon$ , which is periodic in nature:  $T_C \propto -|\epsilon|$ ; thus when one of the sublayers changes its alignment  $-|\epsilon|$  will stay negative. The period of  $\epsilon$  is half the oscillation period of the macro-magnetic observables [2, 21]. The local minima in  $\epsilon$  correspond to uncoupled layers, the maximum - to ferromagnetically or antiferromagnetically coupled layers. The magnetic measurements prove, however, that the structures before

<sup>†</sup> The two calculative methods may result in a difference of  $T_C$  up to 5 degrees. The divergence is the same for all investigated samples within the experimental error - 0.5°.

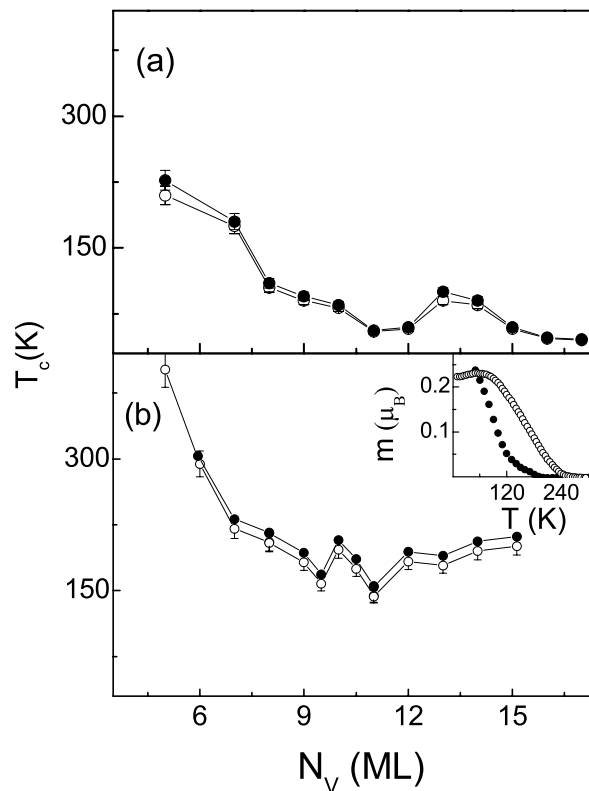


**Fig. 1** The transition temperatures,  $T_c$  versus the number of the vanadium monolayers,  $N_V$ , for (a) Fe(2 ML)/V( $x$  ML) and (b) Fe(2 ML)/V( $y$  ML)/Fe(3 ML)/V( $y$  ML). The dark circles represent the values determined by  $M^2(T) \rightarrow 0$  and the open circles - the values determined by the minimum in  $dM(T)/dT$ . The transition temperatures determined by the second method are presented with 5 % error bars. In the inset of Fig. 1 (b) are shown the field-cooled magnetizations for the uncoupled material Fe(2 ML)/V(11 ML)/Fe(3 ML)/V(11 ML) (the dark circles) and the FM material Fe(2 ML)/V(15 ML)/Fe(3 ML)/V(15 ML) (the open circles).

the first local minimum in Fig. 1 (a) or (b) are FM, and so are the structures after the second local minimum. Thus an increase in  $T_C$  to a local maximum (and respectively in  $\epsilon$ ) can correspond to reversal of the magnetic alignment of one of the sublayers. For the Fe(2 ML)/V( $y$  ML) system this leads to an assumption that neighboring Fe(2 ML) layers may be oppositely aligned for  $N_V$  between 12 and 14 ML, and for Fe(2 ML)/V( $y$  ML)/Fe(3 ML)/V( $y$  ML) - these are possibly the samples with  $N_V$  between 9.5 and 11 ML. The results displayed in Fig. 1 allow to make some observations and conclusions: e. g. the temperature of the local maximum,  $T_C^{max}$ , in Fig. 1 (a) is  $\approx 110$  K, and from Fig. 1 (b) for the interleaved system is seen that  $T_C^{max}$  is  $\approx 210$  K. It is reported in Ref. [16] for Fe(3 ML)/V( $y$  ML) that the range of the AF coupling is 12 – 14 layers of V, and the  $T_C$  of Fe(3 ML)/V(13 ML) is above 300 K. The strengths of the AF coupling can be estimated roughly using the results in Fig. 1 and a simple assumption that the IEC energy  $I \equiv k_B(T_C^{max} - T_C^{min})$ , where  $T_C^{min}$  is the transition temperature of the uncoupled layers.

(This estimate is not quite precise, as it is based on the assumption that all Fe atoms are equally affected by the interlayer coupling; in reality only a part of them experience the maximum coupling strength, which determines the  $T_C$ .) Thus for Fe(2 ML)/V(y ML)  $I$  is  $22.5 \text{ mJ/m}^2$  and for Fe(2 ML)/V(y ML)/Fe(3 ML)/V(y ML)  $I$  is  $31 \text{ mJ/m}^2$ . This leads to the conclusion that adding one Fe monolayer, i. e. effectively one half of an Fe ML in Fe(2 ML)V(13 ML) causes an increase in the coupling energy of 38 %.

In Fig. 2 left panel are shown the magnetic remanences at 20 K:  $M_r/M_s$  of Fe(2 ML)/V(y ML) in Fig. 2 (a) and  $M_r/M_s$  of Fe(2 ML)/V(y ML)/Fe(3 ML)/V(y ML) in Fig. 2 (b). ( $M_s$  is the saturation magnetization of a sample at 20 K.)

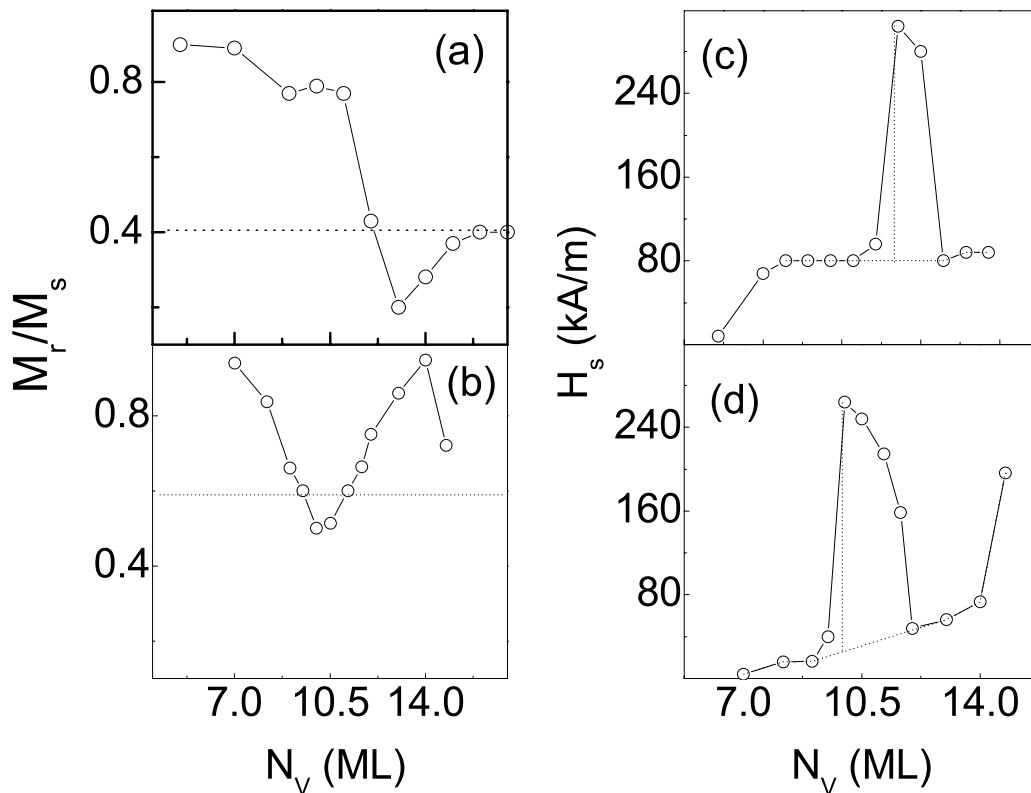


**Fig. 2** Left panel: The magnetic remanence  $M_r/M_s$  versus the number of the V monolayers,  $N_V$ , for (a) Fe(2 ML)/V(y ML) and (b) Fe(2 ML)/V(y ML)/Fe(3 ML)/V(y ML). The dashed horizontal lines in Fig. 2 (a) and (b) are the remanence of the uncoupled layers. Right panel: The saturation fields  $H_s$  as a function of  $N_V$  for Fe(2 ML)/V(y ML) - (c) and Fe(2 ML)/V(y ML)/Fe(3 ML)/V(y ML) - (d). The base dash - lines mark the behavior expected without interlayer coupling. The vertical dash-lines show how the estimate of  $H_{av}$  is made. The solid lines in the figure are guides for the eye. All displayed results are for 20 K.

It is observed in Fig. 2 that the  $M_r/M_s$  drops down to 0.2 in the Fe(2 ML)/V(y ML) system, and it decreases to 0.5 in Fe(2 ML)/V(y ML)/Fe(3 ML)/V(y ML). Results indicate that the remanence of Fe(3 ML)/V(y ML) at 20 K is 0.16 [16]. It makes sense to assume that the additional  $\approx 0.3$  parts of the remanence in Fe(2 ML)/V(y ML)/Fe(3



ML)/V(y ML) are caused by the supplementary Fe monolayer interleaved in this material. The ranges of the V thicknesses to observe the minimum in  $M_r/M_s$  are closely the same as the ranges for the maximum in  $T_C(N_V)$ : 12 - 14 ML for Fe(2 ML)/V(y ML) and 9.5 - 11 for Fe(2 ML)/V(y ML)/Fe(3 ML)/V(y ML). The remanent 0.2 parts in Fe(2 ML)/V(13 ML), and the non-vanishing part of the remanence in these systems in general, are explained with specifics of the fabrication procedure: roughness at the interface of  $\approx 0.5$  ML, ineffective control of the thickness through the repetitive layers and local fluctuations in the thickness, which may result in interface regions with ferromagnetism coexisting with the major AF coupling. Higher values of remanence (0.6) are reported in Ref. [2] for Ni/Au fabricated by sputtering in 10 repetitions, and (-1) in Ref. [11] for Fe/V(001) fabricated by magnetron sputtering in 20 sequences.

In Fig. 2 right panel are displayed the dependencies of the saturation magnetization fields,  $H_s$ , on the thicknesses of the V spacers: in Fig. 2 (c) for Fe(2 ML)/V(y ML) and in Fig. 2 (d) for Fe(2 ML)/V(y ML)/Fe(3 ML)/V(y ML). Two things are noticed straightforward in Figs. 2(c) and (d): the values of the highest saturation fields and their corresponding spacer thicknesses. The maximum saturation field,  $H_s^{max}$ , is  $\approx 280$  kA/m for Fe(2 ML)/V(13 ML), and 260 kA/m for Fe(2 ML)/V(10 ML)/Fe(3 ML)/V(10 ML). The difference of 20 kA/m ( $\approx 250$  Oe) seems rather an artifact like the plateau at 80 kA/m starting at 9 ML of V in Fig. 2 (c). Moreover, the result in Fig. 2 (d) - the  $H_s$  of the materials with V thicknesses above 11 ML also suggests that one reason for the artifact can be the fabrication procedure, another, however, - the interplay between the magnetoelastic forces and the strains at the Fe/V interface. It is also observed in Fig. 2 right panel that the spacer thicknesses,  $N_V$ , which require the highest fields to saturate the samples coincide with the minima in  $\frac{M_r}{M_s}(N_V)$  in Figs. 2 (a) and (b) and the maxima in  $T_C(N_V)$  in Figs. 1 (a) and (b). The saturation field of a material in these systems is the field needed to align both sublayers in one and the same direction; in primarily antiferromagnetic configurations these fields will be the highest,  $H_s^{max}$ . It is not unusual for these structures, and particularly for the AF coupled sublayers, that the saturation fields decrease when the Fe coverage increases (see e.g. the inset of Fig. 4 in Ref. [15]a)<sup>‡</sup>. The basic acting components in an Fe(x ML)/V(13 ML) system are the strains or stresses at the interface, the magnetoelastic forces (surface and volume) and the dipolar (demagnetizing) forces related to the shape anisotropy. At higher Fe coverage the volume magnetoelastic anisotropy becomes relevant, along with the dipolar forces. Their increased relative weights can contribute to the easier alignment of the sublayers in the direction of the magnetic field, and hence the sample's lower saturation fields. The induced magnetic moment in the V spacer [22] is oppositely aligned to the primary Fe monolayers. It contributes to the surface-interface factors acting in favor of high saturation fields.

An  $H_s(N_V)$  - plot allows also to calculate the IEC-energy per unit area, I, for the AF alignment. The estimate is made by interpolating the  $H_s(N_V)$  - points for the

<sup>‡</sup> the relevant measurements in Ref. [15]a are made in the hard-magnetization direction [110] of the samples, the Fe coverage is above 3 ML.

ferromagnetically and uncoupled Fe layers and assuming an effective applied field on the AF structure  $H_{eff} = H_s^{max} - H_{av}$ . The field  $H_s^{max}$  is the maximum in Fig. 2 (c) or (d), and  $H_{av}$  is the estimated average field at the V thickness corresponding to  $H_s^{max}$ , with the Fe layers assumed uncoupled. (The interpolation and method of fitting of the base  $H_s(N_V)$ -plot can cause a divergence of the results of up to 10 %.) These calculations resulted in  $I = 0.0075 \text{ mJ/m}^2$  for the antiferromagnetically coupled Fe(2 ML) sublayers in Fe(2 ML)/V(13 ML), and  $0.05 \text{ mJ/m}^2$  for the Fe(2 ML) and Fe(3 ML)- sublayers in Fe(2 ML)/V(10 ML)/Fe(3 ML)/V(10 ML). This means that adding one Fe ML, or symmetrically 1/2 ML of Fe to Fe(2)/V(13), may cause its IEC to increase  $\approx 6.7$  times. At 13 ML of V, the calculated value of I for Fe(3 ML)/V(13 ML) is  $0.042 \text{ mJ/m}^2$  in Ref. [15]a, and the values for Fe(5 ML)/V(13 ML), Fe(6 ML)/V(13 ML) and Fe(9 ML)/V(13 ML) are  $0.085$ ,  $0.095$  and  $0.055 \text{ mJ/m}^2$ , correspondingly [15]a. These results are displayed in Fig. 3.

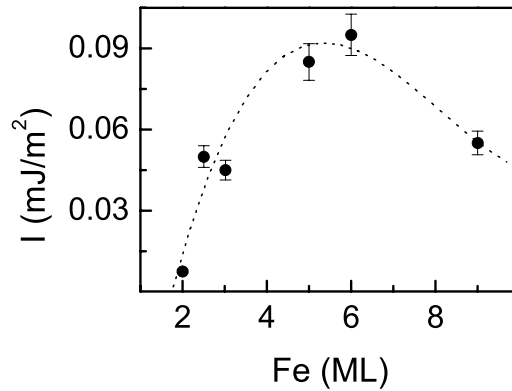


**Fig. 3** Coupling energy I vs. Fe thickness at 13 MLs of V spacer. The dot-line is a third order polynomial regression. Added are 5 % calculation errors to account for the error in the geometric dimensions of the sample, inhomogeneity of the deposition and the errors in the dimensions of the layers.

The maximum coupling strength is reached at  $\approx 5.5$  ML of Fe. It is observed in Fig. 3 that I is not linearly dependent on the thickness of the magnetic layer even at low Fe coverage. (The dot-line in the figure is a third-order polynomial regression - best-fit of the data-points.) The calculations of the IEC energy by this method depend on the Fe thickness in the structure, the saturation magnetization of the sublayers and their respective fields ( $I = \mu_0 M_s H_s x / 4$  [21, 23]). While the magnetization of the layers increases with Fe coverage, the saturation field of the heterostructure may begin to decrease as seen in the inset of Fig. 4 of Ref. [15]a. Thus there is a point in the (I, Fe thickness)-plane, at which the product  $M_s \cdot H_s$  reaches a maximum; after it the increase in  $M_s$  may not compensate for the decrease in  $H_s$ .

The values of I obtained in this work and in Ref. [15]a are low compared to the theoretically calculated ( $0.4 \text{ J/m}^2$ ) in Ref. [1], which deals with smaller spacer thickness (4.5 ML) and the first AF coupling peak. In this work and in Ref. [15] the observed AF coupling is the second, because the expected first coupling and the peak at  $y \approx 3$  ML [9]



are not observed due to the transient ferromagnetic moment in the V spacer [11].

### 3.2 Magnetotransport properties

When a magnetic field is swept through an AF structure aligned in its direction, the electric resistance of the material will change, because it undergoes a magnetic rearrangement. At the field-points of magnetic saturation displayed in Figs. 2 (c) and (d) is expected that the rearrangement is basically completed and the measured resistances will tend to stable minimum values situated on a plateau. The electric current can be pointed in various directions of the sample - in-plane and out-of-plane, to check for magnetoresistive anisotropy. The magnetoresistance ratio is defined as  $MR = \frac{R(0) - R(H_s)}{R(0)}$ , where  $R(H_s)$  is the resistance achieved in the saturation magnetic field and  $R(0)$  is the resistance in zero applied magnetic field. Numerous works including this have verified that the MR is dependent on the temperature and the number of the repetitions: it is higher at lower temperatures and when the structure is repeated consecutive times. A theoretical work proves that the magnitude of the MR depends on the ratio of the mean-free path of the charge carriers to the layer thickness, and depends also on the asymmetry in scattering from spin-up and spin-down electrons [24].

The magnetic field in these experiments was swept up and down to  $\pm 3.5$  T to saturate the materials.

The two series of samples were measured and the dependence of the MR on the  $N_V$  at 10 K was displayed in Fig. 4. The dark circles present the MR of Fe(2 ML)/V(y ML) and the open circles - the MR of Fe(2 ML)/V(y ML)/Fe(3 ML)/V(y ML). It is observed in Fig. 4, for both series of samples, that the ferromagnetic materials exhibit very low MR - practically zero, and that of the uncoupled samples is low as well - below 1 %. As expected, the highest MR is achieved in the samples with AF coupling:  $12 \leq N_V \leq 14$  in Fe(2 ML)/V(y ML) and  $9.5 \leq N_V \leq 11$  in Fe(2 ML)/V(y ML)/Fe(3 ML)/V(y ML). The reported MR of Fe(3 ML)/V(13 ML) at 10 K is 3 % [15]b. In the inset of Fig. 4 is shown the MR as a function of the V thickness with 5 % error bars of the data points. The three points at low Fe coverage are subject to a good linear regression. Thus when the strains at the interface are governing the growth process, the MR is linearly dependent on the Fe thickness. The open circles in the inset of Fig. 4 represent the results for the MR at other Fe thicknesses; the results are taken from Ref. [15]b and the measurements are made with electric current and magnetic fields in the easy magnetization direction [100] of the samples. The results in Fig. 4 confirm that the MR, similarly to the magnetic properties discussed, is dependent on both: the Fe coverage and the spacer thickness. Its highest values are observed at 13 ML of V in the Fe-symmetric Fe(x)/V(y)/MgO(001) materials [15, 21]. It, however, increases linearly only at lower Fe coverage ( $\leq 3$  ML); above 3 ML the dependence is not linear and it has a local maximum at  $N_{Fe} \simeq 5.5$  ML. The decrease of the MR after 5.5 ML of Fe is possibly caused by anisotropy other than the stresses at the substrate/Fe and Fe/V interface. This additional anisotropy may influence the interplay of the basic forces in the system more significantly at Fe coverage above

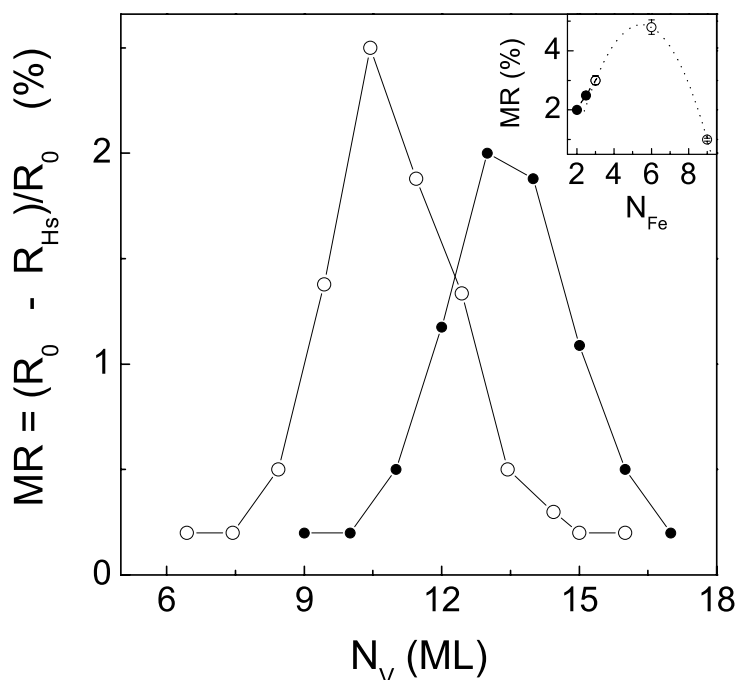


**Fig. 4** The magnetoresistance ratio, MR, vs. vanadium thickness for Fe(2 ML)/V(y ML) (dark circles) and Fe(2 ML)/V(y ML)/Fe(3 ML)/V(y ML) (open circles), both measured at 10 K. The lines are visual guides. In the inset is presented the MR vs. the  $N_{Fe}$  for some measured samples. The dot-lines, presented as one in the inset, are linear regression for  $2 \leq N_{Fe} \leq 3$  and 2-order polynomial for  $N_{Fe} \geq 3$  ML.

5.5 ML. It may also be the cause for the observed decline in the magnetic properties.

## 4 Discussion and conclusions

The investigated systems were grown on MgO(001) substrates, which have fcc crystal structure and lattice constant  $a = 4.212 \text{ \AA}$ . Bulk Fe has bcc  $A_2$  structure and lattice constant  $a = 2.87 \text{ \AA}$ , bulk V has similar crystallographic structure and lattice constant  $3.02 \text{ \AA}$ . There are basically two ways to perform the growth: using a thick buffer layer, e.g. V, or pseudoepitaxial growth of the Fe/V superlattices in the [110] direction of the substrate. In this work was chosen the second approach - the [100] Fe planes were in the [110] MgO direction. The values of the lattice parameters imply that there are considerable misfits, which cause stresses at the surfaces: substrate/Fe interface (misfit  $\approx 36 \%$ ) and Fe/V ( $\approx 5 \%$ ). The stresses are usually accommodated by dislocations above a critical thickness,  $t_c$ , of the material. The first stage of the growth is pseudomorphic to the critical thickness. Above  $t_c$  the growth is relaxed and incoherent with the substrate, the misfit dislocations are stable and the residual strains or stresses drop off at a high rate. E.g.  $t_c$  is  $27 \text{ \AA}$  for Ni grown in Cu/Ni/Cu/Si(001), and the strains decrease as the  $-2/3$  power of the Ni thickness [25].

In a thin film generally, there are five basic factors influencing significantly its behavior and macro-properties: interface, magnetoelastic (ME), elastic, shape and magnetocrystalline anisotropies. They jointly contribute to the effective anisotropy energy density of the thin film,  $K^{eff}$ . It is tempting to observe the interplay of these components, which vary at low and high Fe coverage. In the spin-pair model, which describes the magnetic interaction potential between two atoms with Legendre polynomial [26], the total magnetic anisotropy energy includes the second-order magnetoelastic terms, and is presented as [25]:

$$K^{eff}t = 2(K_N + B_I e_0 + D_I e_0^2) + [B_1(1 + \frac{2c_{11}}{c_{12}}) - D_B e_0]e_0 t - 2\pi M_s^2 t. \quad (1)$$

The term  $2(K_N + B_I e_0 + D_I e_0^2)$  reflects the surface components,  $[B_1(1 + \frac{2c_{11}}{c_{12}}) - D_B e_0]$  - the bulk components and  $-2\pi M_s^2$  is the magnetic contribution of the shape anisotropy. In more detailed presentation,  $B_I$  and  $D_I$  are the **interface** ME coefficients - linear and second-order, correspondingly,  $K_N$  is the Neel-type interface term,  $B_1$  and  $D_B$  - the **bulk** ME coefficients - linear and second-order, respectively,  $M_s$  - the saturation magnetization,  $c_{11}$  and  $c_{12}$  - the elastic constants of the material,  $e_0$  - the biaxial in-plane strain or stress,  $t$  - the thickness of the deposited magnetic material - Fe in the case. Eq. (1) can be presented in a simple form:

$$K^{eff}t = [-a + b\varepsilon(t)]t + C, \quad (2)$$

where the denotations are substitutes of combinations of the physical parameters introduced above. Analysis performed in Ref. [25] shows that at some thickness of the deposited material the contribution of the negative terms in Eq. (1) and (2) can be significant, which will lead to a local maximum in the  $K^{eff}t$  vs.  $t$  dependence. This is possible when the negative-sign terms in Eq. (1), such as the second-order bulk magnetoelastic energy and shape anisotropy become with significant weight over the surface terms. E.g. the second-order bulk magnetoelastic energy is  $\approx 40\%$  of the total anisotropy energy in a 30 Å Ni film in Cu/Ni/Cu/Si(001) [25]a. The position of the maximum in  $K^{eff}t(t)$  on the  $t$ -axis is identified with the critical thickness  $t_c$ , after which the contribution of the bulk magnetoelastic forces is considerable. The Fe/V/MgO(001) superlattices have a substantial shape anisotropy ( $\approx 70 \mu\text{eV}/\text{atom}$ ) favoring in-plane magnetization [13]b. Ref. [13] attempts to obtain experimentally by ferromagnetic resonance methods some of the anisotropy constants for Fe(4 ML)/V(4 ML)/MgO(001). An important conclusion in Ref. [13]b states that the competition between the surface and volume anisotropies results in an unusual temperature dependence of the total fourfold in-plane anisotropy, changing the easy axis of magnetization from [100] to [110] at temperatures higher than the room temperature.

This work investigates Fe(x)/V(y)/MgO(001) materials with low Fe coverage and  $N_V$  between 4 and 17 ML. The Fe growth is limited to the case below the critical thickness  $t_c$ . The Fe monolayers are stressed on the MgO(001) substrate and the elastic parameters in Eq. (1) are approximately constant. The magnetic measurements were made mostly

in the [100] direction though the in-plane magnetic isotropy was confirmed in all investigated materials. The coupling is oscillatory and antiferromagnetism is observed between 12 and 14 MLs of V in Fe(2 ML)/V(y ML)/MgO(001) and 9.5 and 11 MLs of V in Fe(2 ML)/V(y ML)/Fe(3 ML)/V(y ML)/MgO(001). The results displayed in Fig. 3 and Fig. 4 show that at low Fe coverage the IEC depends non-linearly on the Fe thickness and the MR linearly on it. At 5.5 ML of Fe the IEC energy  $I$  and the MR have local maxima. There is a direct dependence of the magnetization on the total anisotropy of the material [13, 25], which suggests a possibility that at 5.5 ML of Fe the volume magnetoelastic anisotropy may begin to overweight in the interplay of the basic contributing factors in the total anisotropy. Macroscopically this may result in changing the equilibrium orientation of the magnetization from [100] to [110], which is in fact observed for thick Fe/V superlattices [13–15].

## Acknowledgment

Dr. A.-M. Blixt from the Department of Materials Physics, Royal Institute of Technology in Stockholm, Sweden is acknowledged for fabricating the materials and numerous discussions.

## References

- [1] P. Bruno and C. Chappert: “Oscillatory coupling between ferromagnetic layers separated by a nonmagnetic metal spacer”, *Phys. Rev. Lett.*, Vol. 67, (1991), pp. 1602–1605; P. Bruno: “Theory of interlayer exchange interactions in magnetic multilayers”, *J. Phys.: Condens. Matter*, Vol. 11, (1999), pp. 9403–9419.
- [2] G. Bayreuther, F. Bensch and V. Kottler: “Quantum oscillations of properties in magnetic multilayers (invited)”, *J. Appl. Phys.*, Vol. 79, (1996), pp. 4509–4514; M.D. Stiles: “Interlayer exchange coupling”, *J. Magn. Magn. Mater.*, Vol. 200, (1999), pp. 322–337.
- [3] Shi Zhupei, Mao Ming and Leng Qunwen: “Method for manufacturing a GMR spin valve having a smooth interface between magnetic and non-magnetic layers”, *US Patent*, No 6479096, B1, 11/12/2002.
- [4] B. Hjörvarsson, J.A. Dura, P. Isberg, T. Watanabe, T.J. Udovic, G. Andersson and C.F. Majkrzak: “Reversible Tuning of the Magnetic Exchange Coupling in Fe/V (001) Superlattices Using Hydrogen”, *Phys. Rev. Lett.*, Vol. 79, (1997), pp. 901–904.
- [5] R.H. Victora, Wenbin Peng, Jianhua Xue and J.H. Judy: “Superlattice magnetic recording media: experiment and simulation”, *J. Magn. Magn. Mater.*, Vol. 235, (2001), pp. 305–311.

- [6] (a) C.F. Majkrzak, J. Kwo, M. Hong, Y. Yafet, D. Gibbs, C. L. Chein and J. Bohr: “Magnetic rare earth superlattices”, *Adv. Phys.*, Vol. 40, (1991), pp. 99–189;  
(b) J.J. Rhyne and R.W. Erwin: *Magnetic Materials*, Vol. 8, ed. K.H.J. Buschow, Amsterdam, North Holland, 1995.
- [7] (a) J. Unguris, R.J. Celotta and D.T. Pierce: “Observation of two different oscillation periods in the exchange coupling of Fe/Cr/Fe(100)”, *Phys. Rev. Lett.*, Vol. 67, (1991), pp. 140–143;  
(b) E.E. Fullerton, S.D. Bader and J.L. Robertson: “Spin-Density-Wave Antiferromagnetism of Cr in Fe /Cr(001) Superlattices”, *Phys. Rev. Lett.*, Vol. 77, (1996), pp. 1382–1385.
- [8] Y. Wang, P.M. Levy and J.L. Fry: “Interlayer magnetic coupling in Fe/Cr multilayered structures”, *Phys. Rev. Lett.*, Vol. 65, (1990), pp. 2732–2735; C. Lacroix and J.P. Gavigan: “Interlayer coupling in magnetic multilayers: analogy to superexchange processes in insulators”, *J. Magn. Magn. Mater.*, Vol. 93, (1991), pp. 413–417.
- [9] M. van Schilfgaarde and Frank Herman: “Simplified first principles approach to exchange coupling in magnetic multilayers”, *Phys. Rev. Lett.*, Vol. 71, (1993), pp. 1923–1926.
- [10] M. Pajda, J. Kudrnovsky, I. Turek, V. Drchal and P. Bruno: “Oscillatory Curie Temperature of Two-Dimensional Ferromagnets”, *Phys. Rev. Lett.*, Vol. 85, (2000), pp. 5424–5427.
- [11] M.M. Schwickert, R. Coehoorn, M.A. Tomaz, E. Mayo, D. Lederman, W.L. O’Brien, Tao Lin and G.R. Harp: “Magnetic moments, coupling, and interface interdiffusion in Fe/V(001) superlattices”, *Phys. Rev. B*, Vol. 57, (1998), pp. 13681–13691.
- [12] (a) Wei Pan, D. Sander, Minn-Tsong Lin and J. Kirschner: “Stress oscillations and surface alloy formation during the growth of FeMn on Cu(001)”, *Phys. Rev. B*, Vol. 68, (2003), art. 224419;  
(b) B.A. Hamad and J.M. Khalifeh: “Magnetism of (Fe, V, Mo)/Pd(0 0 1) systems”, *Surface Sci.*, Vol. 481, (2001), pp. 33–38.
- [13] (a) A.N. Anisimov, M. Farle, P. Pouloupoulos, W. Platow, K. Babershcke, P. Isberg, R. Wäppling, A.M.N. Niklasson and O. Eriksson: “Orbital Magnetism and Magnetic Anisotropy Probed with Ferromagnetic Resonance”, *Phys. Rev. Lett.*, Vol. 82, (1999), pp. 2390–2393;  
(b) A.N. Anisimov, W. Platow, P. Pouloupoulos, W. Wisny, M. Farle, K. Babershcke, P. Isberg, B. Hjörvarsson and R. Wäppling: “The temperature-dependent in- and out-of-plane magnetic anisotropies in superlattices”, *J. Phys.: Condens. Matter*, Vol. 9, (1997), pp. 10581–10593.
- [14] A. Broddefalk, P. Nordblad, P. Blomquist, P. Isberg, R. Wäppling, O. Le Bacq and O. Eriksson: “In-plane magnetic anisotropy of Fe/V (0 0 1) superlattices”, *J. Magn. Magn. Mater.*, Vol. 241, (2002), pp. 260–270.
- [15] (a) A. Broddefalk, R. Mathieu, P. Nordblad, P. Blomquist, R. Wäppling, J. Lu and E. Olsson: “Interlayer exchange coupling and giant magnetoresistance in Fe/V (001) superlattices”, *Phys. Rev. B*, Vol. 65, (2002), art. 214430;

- (b) P. Nordblad, A. Broddefalk, R. Mathieu, P. Blomquist, O. Eriksson and R. Wäppling: “Fe/V and Fe/Co (0 0 1) superlattices: growth, anisotropy, magnetisation and magnetoresistance”, *Phys. B*, Vol. 327, (2003), pp. 344–348.
- [16] P. Isberg: *Preparation and properties of Fe/V Superlattices*, Thesis PhD, Uppsala, Sweden, 1997.
- [17] P. Isberg, B. Hjörvarsson, R. Wäppling, E.B. Svedberg and L. Hultman: “Growth of epitaxial Fe/V (001) superlattice films”, *Vacuum*, Vol. 48, (1997), pp. 483–489.
- [18] J.E.E. Baglin and J.S. Williams: “High Energy Ion Scattering Spectrometry”, In: J.R. Bird and J.S. William (Eds.): *Ion Beams for Material Analysis*, Academic Press, Australia, 1989, pp. 103–148.
- [19] P.V. de Weijer and D.K.G. de Boer: “Glancing-incidence x-ray fluorescence of layered materials”, *Philips J. Res.*, Vol. 47, (1993), pp. 247–249.
- [20] E. Fullerton, I.K. Schuller, H. Vanderstraeten and Y. Bruynseraede: “Structural refinement of superlattices from x-ray diffraction”, *Phys. Rev. B*, Vol. 45, (1992), pp. 9292–9310.
- [21] K. Eftimova, A.M. Blixt, B. Hjörvarsson, R. Laiho, J. Salminen and J. Raitilla: “Magnetic properties and coupling in Fe(2 ML)/V(x ML) ( $x > 5$ ) superlattices”, *J. Magn. Magn. Mater.*, Vol. 246, (2002), pp. 54–61.
- [22] S. Ostanin, V.M. Uzdin, C. Demangeat, J.M. Wills, M. Alouani and H. Dreyse: “Effect of hydrogen on the interlayer exchange coupling in Fe/V superlattices”, *Phys. Rev. B*, Vol. 61, (2000), pp. 4870–4876; L.-C. Duda, P. Isberg, S. Mirbt, J.-H. Guo, B. Hjörvarsson and J. Nordgren: “Soft-x-ray emission study of Fe/V (001) superlattices”, *Phys. Rev. B*, Vol. 54, (1996), pp. 10393–10396.
- [23] P. Grangberg, P. Isberg, E.B. Svedberg, B. Hjörvarsson, P. Nordblad and R. Wäppling: “Antiferromagnetic coupling and giant magnetoresistance in Fe/V(0 0 1) superlattices”, *J. Magn. Magn. Mater.*, Vol. 186, (1998), pp. 154–160.
- [24] R.E. Camley and J. Barnas: “Theory of giant magnetoresistance effects in magnetic layered structures with antiferromagnetic coupling”, *Phys. Rev. Lett.*, Vol. 63, (1989), pp. 664–667.
- [25] (a) Kin Ha and R.C. O’Handley: “Nonlinear magnetoelastic anisotropy in Cu/Ni/Cu/Si(001) films”, *J. Appl. Phys.*, Vol. 85, (1999), pp. 5282–5284;  
(b) D.S. Chuang, C.A. Ballentine and R.C. O’Handley: “Surface and step magnetic anisotropy”, *Phys. Rev. B*, Vol. 49, (1994), pp. 15084–15095.
- [26] S. Chikazumi: *Physics of Ferromagnetism*, 2nd ed., Oxford Science, 1997, p. 350.